

Active flow control by means of plasma actuator in the curvilinear channel

Kazanskiy P., Moralev* I., Firsov *A.A. Semenev** P. A.*

** Joint Institute of High Temperature RAS*

Izhorskaya str.13 bld.2, Moscow, 125412, Russia

*** Central Institute of Aviation Motors*

Aviamotornaya str., 2, Moscow, 111116 Russia,

Abstract

The active flow separation control by means of different plasma actuators was organized in the curvilinear channel. Two main types of plasma actuators were tested. First one was based on dielectric barrier discharge used in PSVG configuration. The significant effect on the flow separation was obtained only at flow velocities less than $V=30$ m/s. The PIV visualization shows that the shift of separation point up to 20mm can be obtained while actuator is switched on. The dynamic pressure distribution was measured at the exit section of the channel. It was shown, that the average pressure loss coefficient is reduces by 10% at PSVG actuator operation at 20m/s. The flow control by means MHD of plasma actuator was successfully implemented at flow velocities up to $V=80$ m/s. At mean discharge power no more than 200 W the velocity of the arc may be up to 250 m/s, providing the comparable disturbances of the flow velocity. At 70m/s, the significant changes in separation region geometry and loss coefficient distribution were obtained for actuator operation at 150Hz repetition rate.

MHD = Magnetohydrodynamics

DBD = Dielectric barrier discharge

PIV = Particle image velocimetry

I = pulsating current

B = magnetic flux density

f = discharge pulse frequency

V = airflow velocity

1. Introduction

The active separation flow control was studied in number of papers. The promising plasma technology is developing rapidly. Several decades ago the DBD actuators seemed to solve the technical problem in high Reynolds number in separation flow control [1-3]. However, the low velocity of the induced jet (less than 10 m/s) [4] allowed the use of the DBD actuator only in limited problems [5]. The use of an MHD actuator [6] is intended to increase the velocity of the induced jet. It can be more efficient vortex generator. In a series of papers [7-16] intensification of mixing was investigated in gas subsonic flow at atmospheric pressure. A great experience was accumulated in investigation of electric arc interaction stirring in a flow by means of Lorentz force $f=[jB]$. Different configuration of MHD actuators based on principals of momentum transfer from arc to the flow were used in previous works of aircraft exhaust engine jet noise control [17]. The current article is intended to demonstrate the possibility of using a plasma actuator in problems [18] of controlling the separation flow in the curvilinear channel at high Reynolds numbers.

2. Experimental setup

Low-velocity (<70m/s) experiments were carried in the aerodynamic curvilinear channel with 100x150 test section, operating in a continuous regime in the wind tunnel «D-2» in JIHT RAS (Fig.1). To stabilize the transition position, the sandpaper with 0.5 grin was mounted at distance of 20mm from the channel entrance.

The measurement equipment included pressure sensors and PIV. The set of pitot tubes was placed in the far field of the channel in terms to measure the total pressure distribution. Several ports were organized on the walls of the wind tunnel for static pressure measurements. The 16 pressure scanner Esterline 9116 was used for signal registration.

The structure of separation region was studied by a LaVision PIV system, based on 200mJ NdYAG laser and a 2048x2048 pix camera. Frames were acquired at frame rate ~ 7 Hz, with further averaging of 50-140 images. Accuracy of a single measurement was about 3% (for 40 m/s), while averaging error was several times higher, velocity field resolution was about 1.5mm. Diagnostic equipment was synchronized with the discharge pulses through the frequency divider and delay generator, allowing phase-locked acquisition of data. During the acquisition of average flowfield, the special care was taken to avoid frequency locking to the discharge repetition rate. Flow was seeded with TiO₂ particles with the typical size 150 nm.

The actuators were mounted in a special insertion in the field of maximum curvature of the channel. The insertion was manufactured by 3D printer. Different elements of construction were placed on it.

The DBD actuator is shown in Fig.2. The electrodes are located on the surface of the insert and are aligned in a downstream direction. The initiated EHD force is directed in spanwise direction (parallel to the wall and perpendicular to the flow). In such configuration the actuator forms the longitudinal cortex pairs, affecting the momentum transfer to the boundary layer. The kapton with a total thickness of 200 μ m was used as dielectric material. The electrodes of 20 μ m were made from copper, 5 mm wide. The distance between electrodes were 10 mm. The power supply was organized using a resonant power source, producing sinusoidal voltage with $f=7$ kHz and $U_a=15$ kV.

The MHD actuator design is shown in Fig.3. The number of tungsten electrodes were placed on the ceramic surface of the insert. The main idea of actuator was acceleration of boundary layer by means of plasma arc channel in cross magnetic field. It was also believed, that such configuration would lead to vortex generation due to the strong vortex source present on the edge of the arc moving in the magnetic field. The permanent magnet was placed inside the insert, providing the field at the position of the discharge on the order of 0.2 T. The sharpeners on electrodes ensured the ignition point of discharge. The distance between electrodes were 8mm. The power supply provided current pulses of sinusoidal shape with 600 μ s duration at repetition rate of 100-200 Hz. The amplitude of the current was 20A.

3.Results and discussion

The structure of the flow in the channel was investigated at velocities up to 70 m/s. The velocity field of the flow at 50 m/s is visualized in Fig.4. It can be seen that the flow separation occurs at a distance of about 22 mm along the surface from the point of maximum curvature.

The influence of DBD vortex generators on the flow separation was studied by PIV and pressure rake. The visualization of separation point shift while DBD plasma actuator at flow velocity of 20 m/s is switched on can be seen in Fig. 4. It is possible to notice, that the turning on the discharge leads to a displacement of the separation point downstream by 15-20 mm, while the thickness of the separation zone decreases.

Fig. 5 shows the distribution of pressure in the central section of the channel at $X = 95$ mm, as well as the dependence of the total pressure loss on the flow velocity. It can be seen that significant changes in the hydraulic resistance of the channel are observed in the velocity range up to 30 m/s. In this range of velocities, the DBD actuator operation leads to a significant (1-2 m/s) increase in the flow velocity in the channel with a constant power of blower engine. With further flow velocity increase there is a section on which a negative effect is observed while the actuator is turned on. At high velocities 60 m/s or more, the actuator does not affect the hydraulic resistance of the channel.

The effect of MHD plasma actuator on the flow control in the curved channel was investigated at flow velocities up to 70m/s. The arc movement was found to be very sensitive to the magnetic field orientation. The design of MHD actuator was corrected after the proper magnetic field modeling, so that the Lorentz force would press the arc against the wall. After that, the actuator effect on the pressure in the far zone $X = 950$ mm was significantly increased.

The oscillograms of the current and voltage of the MHD actuator pulse are shown in Fig.6. The typical current amplitude was $I_a = 20$ A, $t_{imp} = 600$ μ s. The voltage oscillogram shows amplitude rapid decrease after the breakdown ($t=250-500$ μ s); after that the oscillations in the range of 400-800 V are observed, with a characteristic average voltage of 500 V, which is explained by the stepped nature of the discharge motion in an external magnetic field. The average power of the actuator during the pulse was 10 kW, which corresponded to the deposited energy of 3.3 J. The voltage on the discharge capacitance during the operation of the actuator dropped from 3.5 kV to 3.0 kV. Thus, the energy of the capacitance decreased from 61 J to 45 J at 16 J, which makes it possible to estimate the efficiency of matching the power source and the discharge gap to 20%.

It was found that arc discharge ignition leads to velocity field restructuring at the velocities up to 70 m/s. The visualization of separation region is presented in Fig.7. One can see that the MHD actuator operation does not lead to the shift of the separation point. However, the angle of shear layer changes, so that the mean size of the circulation zone reduces.

The result of pressure measurement in far zone $X = 950$ mm is presented in Fig.8. It is clearly seen that the actuator decreases total pressure in Y range 0 - 40 mm, and increases pressure in range 40-140mm. This behavior is assumed to be typical for the separation zone size reduction. Nevertheless, the average pressure loss coefficient was found to increase.

References

1. P. N. Kazanskyi, A. I. Klimov, and I. A. Moralev, "High-frequency actuator control of air flow near a circular cylinder: Impact of the discharge parameters on the cylinder aerodynamic drag," *High Temp.*, vol. 50, no. 3, pp. 323–330, 2012.
2. C. L. Kelley, T. C. Corke, F. O. Thomas, M. Patel, and A. B. Cain, "Design and Scaling of Plasma Streamwise Vortex Generators for Flow Separation Control," *AIAA J.*, pp. 1–12, 2016.
3. Roth J R 2003 *Phys. Plasmas* 10 2117–26
4. Debien A, Benard N and Moreau E 2012 Streamer inhibition for improving force and electric wind produced by DBD actuators *J. Phys. D: Appl. Phys.* 45 215201
5. S. Baleriola, A. Leroy, S. Loyer, P. Devinant, S. Aubrun // Circulation control on a rounded trailing-edge wind turbine airfoil using plasma actuators // *Journal of Physics: Conference Series* 753 (2016) 052001 doi:10.1088/1742-6596/753/5/052001
6. P. N. Kazanskiy, I. A. Moralev, V. A. Bityurin, and A. V. Efimov, "Active flow control on a NACA 23012 airfoil model by means of magnetohydrodynamic plasma actuator," *J. Phys. Conf. Ser.*, vol. 774, p. 12153, 20
7. V.A.Bityurin, A.N.Bocharov, Advanced MHD assisted Mixing of Reacting Streams, In: 39th AIAA Aerospace Sciences Meeting & Exhibit, Reno, NV, 2001, AIAA Paper 2001-0793.
8. A.Bocharov, V.Bityurin, I.Klement'eva, and S.Leonov. Experimental and Theoretical Study of MHD Assisted Mixing and Ignition in Co-Flow Streams // In: 14th International Conference on MHD Power Generation and High Temperature Technologies, Maui, Hawaii, 2002, AIAA Paper 2002-2248.
9. A.Bocharov, V.Bityurin, I.Klement'eva, and S.Leonov, A Study of MHD Assisted Mixing and Combustion, In: 41st Aerospace Sciences Meeting and Exhibit, Reno, NV, 2003, AIAA Paper 2003-5878.
10. A.Bocharov, V.Bityurin, E.Filimonova and A.Klimov, Numerical Study of Plasma Assisted Mixing and Combustion in Non-Premixed Flows, In: 42nd Aerospace Sciences Meeting and Exhibit, Reno, NV, 2004, AIAA Paper 2004-1017.
11. A.Bocharov, I.Klement'eva, A.Klimov, V.Bityurin, A Study of MHD Assisted Mixing and Combustion in Counter-Flow Streams, In: 43rd Aerospace Sciences Meeting and Exhibit, Reno, NV, 2005, AIAA Paper 2005-0600.
12. V.A.Bityurin, A.N.Bocharov, I.B.Klement'eva, A.I.Klimov, Experimental and Numerical Study of MHD Assisted Mixing and Combustion, In: 44th Aerospace Sciences Meeting and Exhibit, Reno, NV, 2006, AIAA Paper 2006-1009.
13. V.Bityurin, I.Klementyeva, A.Bocharov. Investigation of electrical discharges interaction with gas flows in external magnetic fields for problems of mixing and combustion intensification // In: 16th International Conference on Gas Discharges and their Applications, Xian, China, Sept. 11-15, 2006, pp.425 – 428.
14. A.Bocharov, V.Bityurin, I.Klement'eva, A.Klimov. Numerical and Experimental Study of MHD Assisted Mixing and Combustion // In: 45th Aerospace Sciences Meeting and Exhibit, Reno, NV, 2007, AIAA Paper 2007-1024.
15. I. B. Klementyeva, A.Bocharov, V. A. Biturin. Features of interaction of electrical discharge with a gas flow in an external magnetic field // *Letters to the Journal of Technical Physics* T.33. Is.22, 2007, c.16 – 22.
16. I. B. Klementyeva, V. A. Biturin, B. N. Tolkunov, I. A. Moralev Experimental study of electrical discharges in gas flows under external magnetic field // *High Temperature*. December 2011, Volume 49, Issue 6, pp 788-796
17. Moralev I.A., Zhaketov V.D. Interaction of the magnetically driven arc discharge with a mixing layer of a high-velocity turbulent jet // *The 11th International Workshop on Magneto-plasma Aerodynamics*. p 344. 2012.
18. Yu. F. Kashkin, A. E. Konovalov, S. Yu. Krashenninikov, D. A. Lyubimov, D. E. Pudovikov, and V. A. Stepanov. Experimental and Numerical Investigation of Separated Flows in Subsonic Diffusers // ISSN 0015-4628, *Fluid Dynamics*, 2009, Vol. 44, No. 4, pp. 555–565.
19. Kazanskyi, P.N., Klimov, A.I., Moralev, I.A. High-frequency actuator control of air flow near a circular cylinder: Impact of the discharge parameters on the cylinder aerodynamic drag // *High Temperature*. 2012

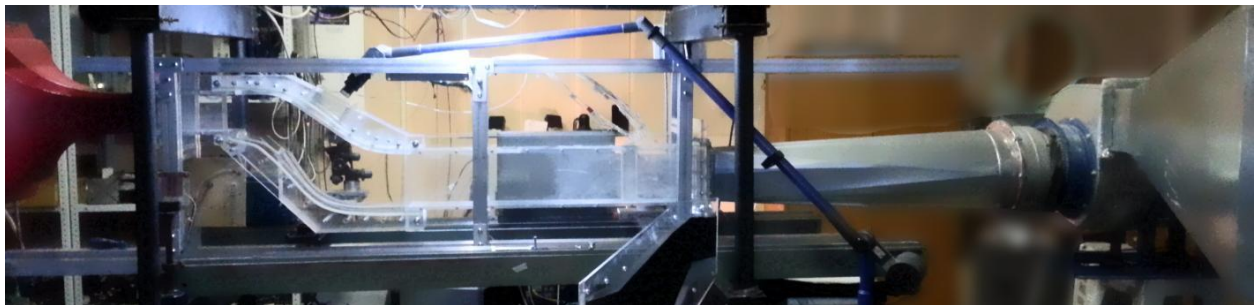
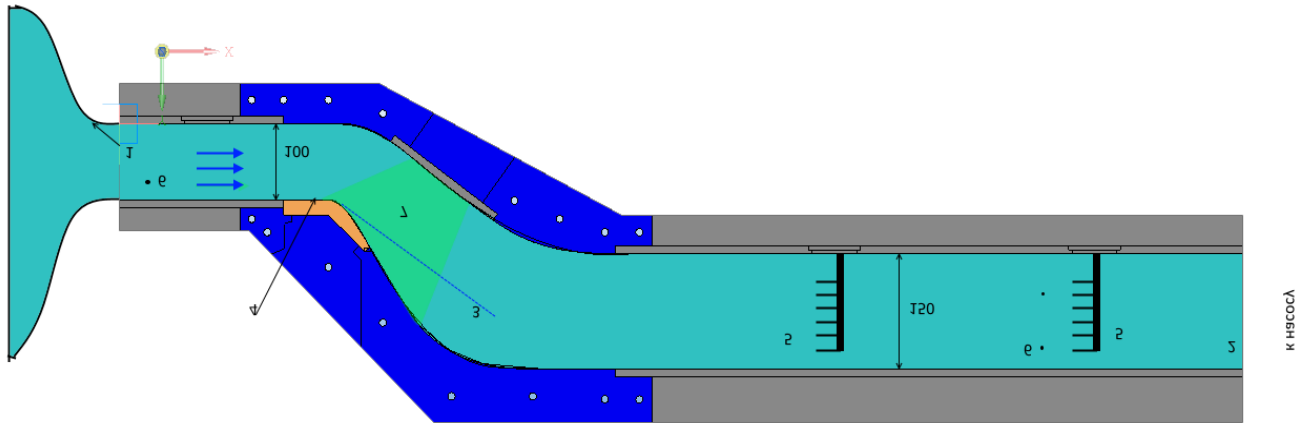


Fig. 1 The scheme of the curvilinear channel D-3 for the flow separation control. 1- nozzle, 2- channel outlet, 3- boundary of the bubble, 4- place of installation of the actuators, 5-combs of full pressure, 6-points of measurement of static pressure, 7-area of PIV measurements.

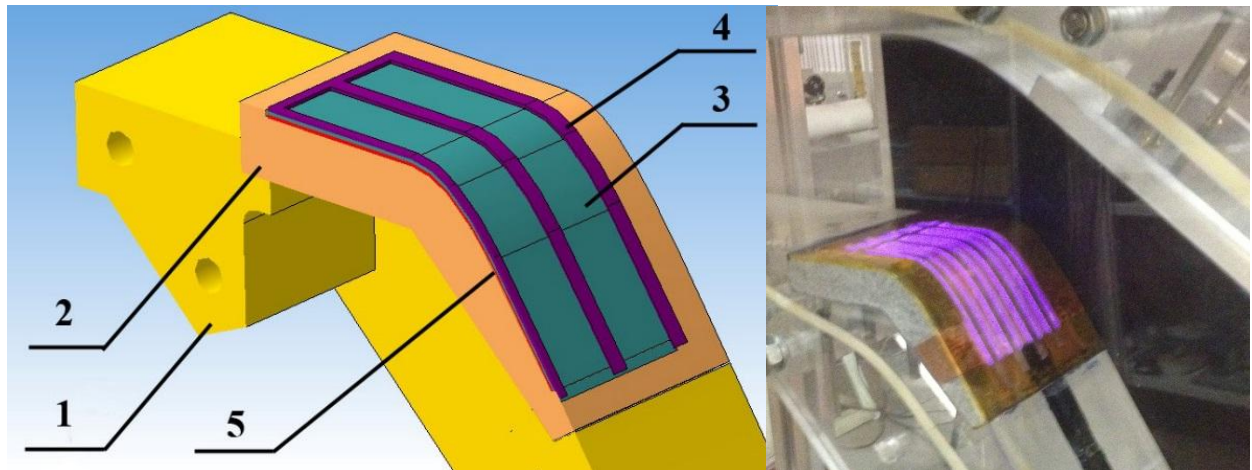


Fig. 2. The DBD actuator insert scheme (left). Photo of the DBD actuator while discharge is on (right). 1 - wall of the wind tunnel, 2 - profile of the wind tunnel, 3 - dielectric plate, 4 - high-voltage electrode, 5 - grounded electrode.

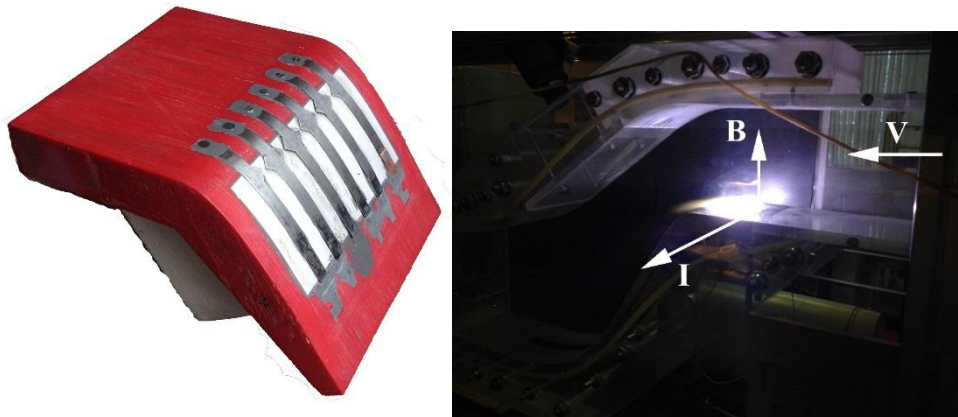


Fig. 3. The MHD actuator in the section.

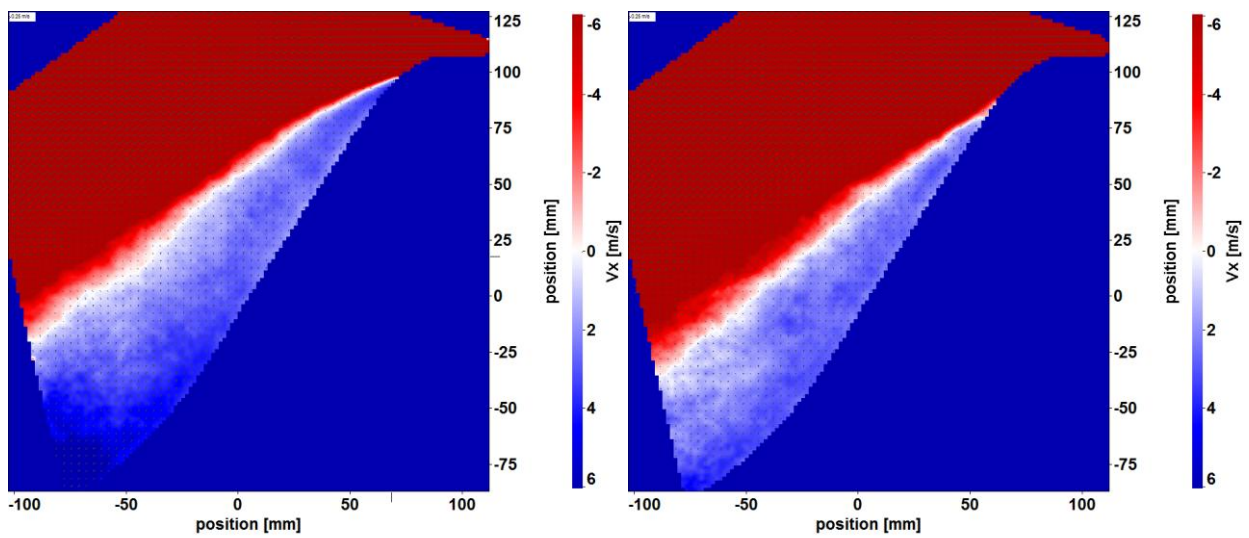


Fig. 4. The DBD plasma actuator flow control visualization by means of PIV. Plasma is off (left). Plasma is on (right). $V = 20 \text{ m/s}$

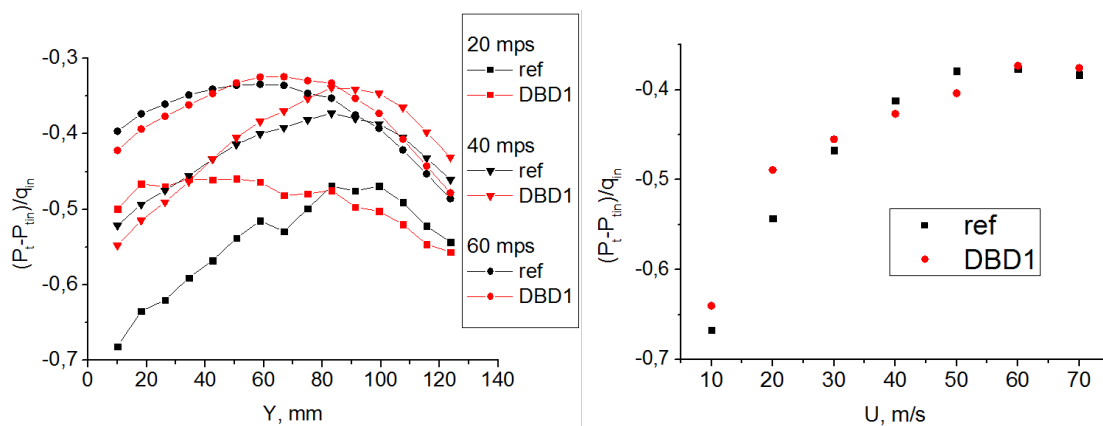


Fig. 5. The total pressure loss coefficient while DBD actuator is switched on. The distribution of the pressure loss coefficient in the central section of the channel (left). The average pressure loss coefficient with and without an operating actuator (right).

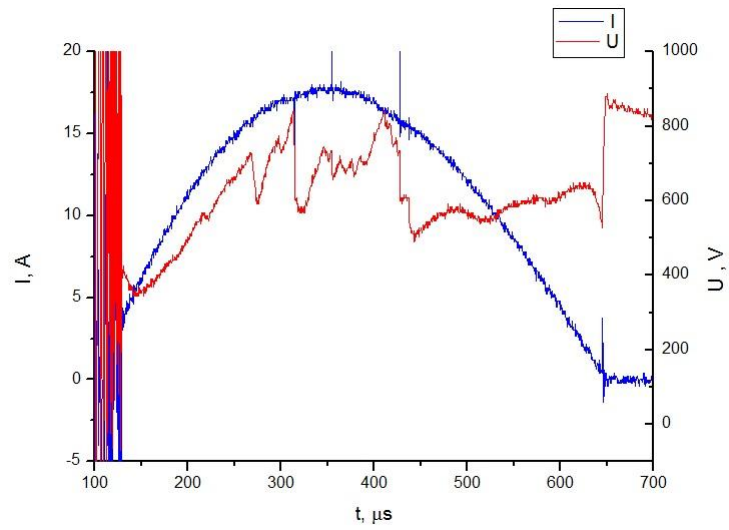


Fig. 6. Current and voltage waveforms of MHD actuator.

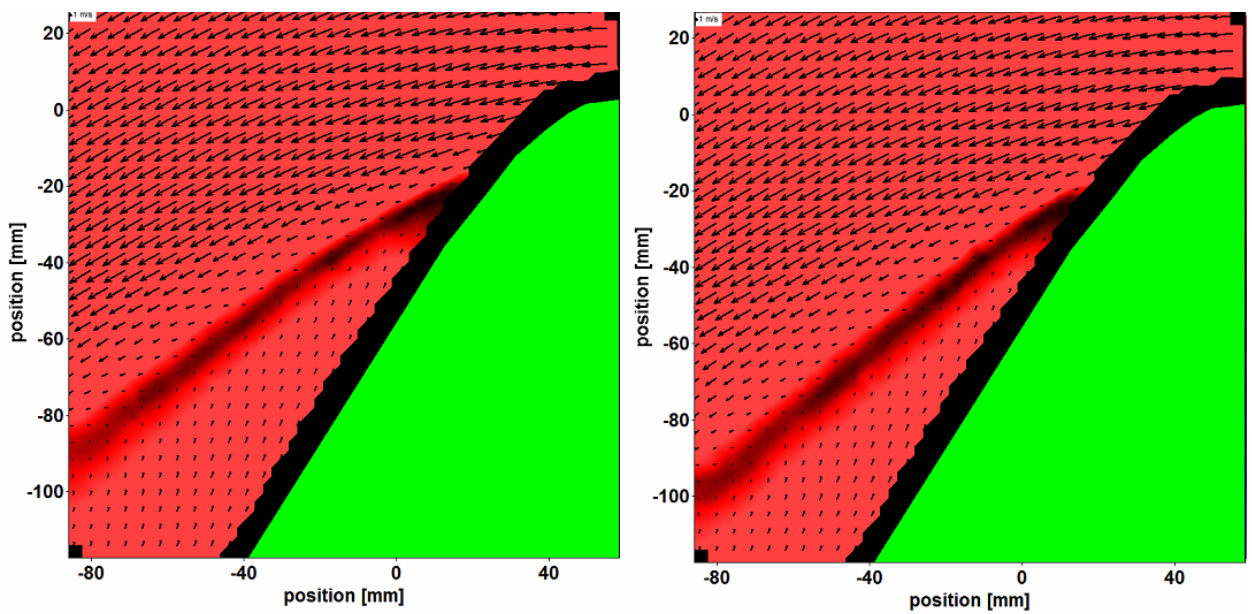


Fig. 7. The MHD plasma actuator flow control visualization by means of PIV. Plasma is off (left). Plasma is on (right). $V = 50 \text{ m/s}$

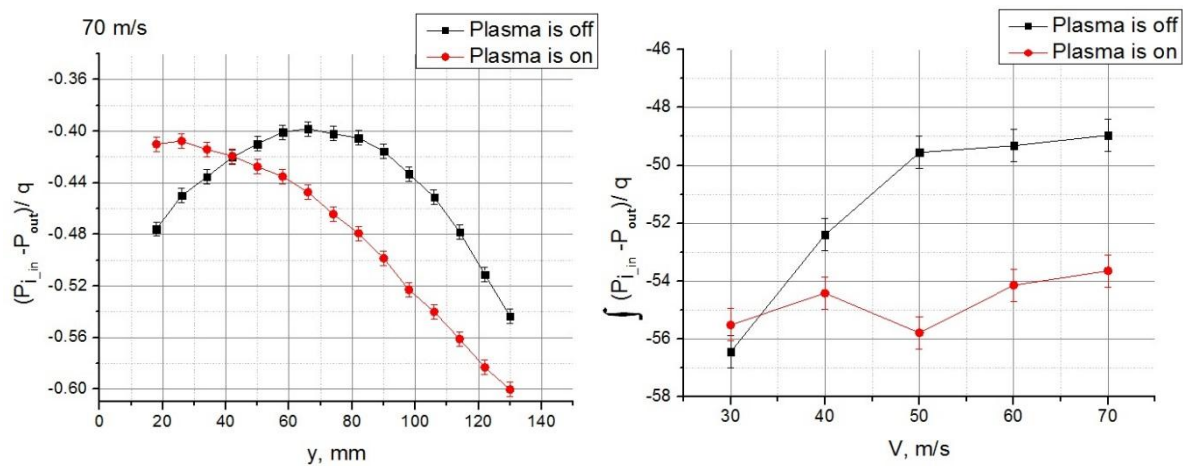


Fig. 8. The total pressure loss coefficient while MHD actuator is switched on. The typical distribution of the pressure loss coefficient in the central section of the channel (left). The average pressure loss coefficient with and without an operating actuator (right).